DOE/NASA/0394-1
NASA CR-174755

Computer Simulation of the Heavy-Duty Turbo-Compounded Diesel Cycle for Studies of Engine Efficiency and Performance

Dennis N. Assanis, Jack A. Ekchian,
John B. Heywood, and Kriss K. Replogle
Sloan Automotive Laboratory
Massachusetts Institue of Technology
Cambridge, Massachusetts 02139

May 1984

Prepared for
NATIONAL AERONAUTICS AND SPACE ADMINISTRATION
Lewis Research Center
Cleveland, Ohio 44135
Under Grant NAG 3-394

for
U.S. DEPARTMENT OF ENERGY
Conservation and Renewable Energy
Office of Vehicle and Engine R&D
Washington, D.C. 20585
Under Interagency Agreement DE-AI01-80CS50194

Table of Contents

11. PROGRAM INPUTS AND OUTPUTS

1. INTRODUCTION

The use of ceramics in heavy duty diesel engine applications is especially promising [1]. It has been shown in the TACOM/Cummins Adiabatic Engine Program that reductions in heat losses at appropriate points in the diesel engine system result in substantially increased exhaust enthalpy [2]. One of the most promising concepts for taking advantage of this increased exhaust enthalpy is the turbocharged turbo-compounded diesel engine cycle [3].

This engine concept consists of several sub-systems: compressor, engine, turbocharger turbine, compounded turbine, ducting and heat exchangers. Applications of ceramic materials to different sub-system components have widely different degrees of difficulty. Therefore, there is a need for a computer simulation of this engine concept, at the appropriate level of detail, to enable engineers to define the trade-offs associated with introducing ceramic materials in various parts of the total engine system, and to carry out system optimization studies.

This report describes the model being developed for simulating the behavior of the total engine system. The focus of this total system simulation is to define the mass and energy transfers (heat transfers, heat release, work transfers) in each sub-system and the relationship between the sub-systems. Since this system model must function as a single-unit, in this development program, a deliberate effort is made to maintain a balance in the complexity of the various sub-system descriptions.

Figure 1 illustrates the proposed overall model structure. The air flow is followed through an air filter, ducting, turbocharger compressor, ducting, cooler and engine intake system, to the diesel engine. The engine operating cycle is then modelled. The exhaust gas flow is followed through the engine exhaust ports, manifold and ducting to the turbocharger turbine; then followed

through additional ducting to the compounded turbine, the exhaust system and muffler to the atmosphere. Engine friction sub-models are then used to obtain brake quantities from the computed indicated quantities.

The engine model of the total system simulation is a mathematical model of the processes occuring in a diesel engine over a complete cycle. The direct-injection four-stroke diesel-engine cycle-simulation developed in this work is based on two existing M.I.T. engine cycle simulations: (i) a spark-ignition engine simulation [4], and (ii) a divided-chamber diesel engine simulation [5]. The direct-injection diesel simulation has retained many of the basic modelling assumptions (gas exchange process, thermodynamic and transport properties routines), as well as the modular structure and efficient computational algorithm of the parent codes.

The tasks in the first year of the program were to develop this DI diesel simulation, modify this single cylinder engine model to predict the performance of a multi-cylinder engine, and to implement the appropriate logic for coupling the multi-cylinder engine with the turbocharger, compound turbine and other system component models.

The purpose of this report is to summarize the basic assumptions and mathematical relationships used in this simulation of the turbocharged turbo-compounded diesel engine cycle. The report is arranged as follows. Sections 2, 4 and 5 describe the simulation of the diesel engine itself. Sections 6 and 7 describe the models used for the other system components: the turbocharger compressor and turbine, compound turbine, wastegate, cooler, manifold and ducting models. Sections 3, 8 and 9 relate to all parts of the total engine system. Sections 10 and 11 describe the integration together of all the subsystems, and program inputs and outputs.

2. BASIC ASSUMPTIONS OF ENGINE MODEL

The diesel engine cycle is treated as a sequence of continuous processes: intake, compression, combustion (including expansion), and exhaust. The duration of the individual processes are as follows. The intake process begins when the intake valve opens (IVO) and ends when the intake valve closes (IVC). The compression process begins at IVC and ends at the time of ignition (IGN). The combustion process begins when ignition occurs and ends when the exhaust valve opens (EVO). The exhaust process begins at EVO and ends at IVO (and not when the exhaust valve closes).

In the engine simulation, the system of interest consists of the instantaneous contents of a cylinder, i.e. air and combustion products. In general, this system is open to the transfer of mass, enthalpy, and energy in the form of work and heat. Throughout the cycle, the cylinder is treated as a variable volume plenum, spatially uniform in pressure. Furthermore, the cylinder contents are represented as one continuous medium by defining an average equivalence ratio and temperature in the cylinder at all times.

Gas properties are obtained assuming ideal gas behavior. At low temperatures (below 1000 K), the cylinder contents are treated as a homogeneous mixture of non-reacting ideal gases. At high temperatures (above 1000 K), the properties of the cylinder contents are calculated with allowance for chemical dissociation by assuming that the burned gases are in equilibrium, using an approximate calculation method based on hydrocarbon air combustion.

Quasi-steady, adiabatic, one-dimensional flow equations are used to predict mass flows past the valves. The intake and exhaust manifolds are treated as plenums whose pressure and temperature histories are determined by solution of the manifold state equations. When reverse flow past the intake

valve occurs, a rapid mixing model for the back flow gases is assumed. The engine model couples with the compressor and heat exchanger at the inlet manifold, and with the turbocharger turbine at the exhaust manifold.

The compression process is defined so as to include the ignition delay period; i.e., the time interval between the start of the injection process (the point at which the injector needle starts to lift) and the ignition point (the start of positive heat release due to combustion). The total length of the ignition delay is related to the mean cylinder gas temperature and pressure during the delay period by an empirical Arrhenius expression.

The combustion process is modelled as a uniformly distributed heat release process. The rate of heat release is assumed to be proportional to the rate of fuel burning which is modelled empirically. Since the diesel combustion process is comprised of a pre-mixed and diffusion-controlled combustion mechanism, it was decided to use Watson's fuel burning rate correlation [6], consisting of the sum of two algebraic functions, one for each combustion mechanism. The proportion of the total fuel injected that is burnt by either mechanism depends on the length of the ignition delay period and the engine load and speed.

Heat transfer is included in all the engine processes. Convective heat transfer is modelled using available correlations for turbulent flow in pipes. The characteristic velocity and length scales required to evaluate these correlations are obtained from a mean and turbulent kinetic energy model. Radiative heat transfer is added during combustion.

Finally, an empirical friction model is used to convert the indicated engine performance quantities to brake performance quantities.

3. CONSERVATION EQUATIONS

In this section, equations for the conservation of mass and energy will be stated for the contents of a generalized control volume treated as an open system. The conservation equation for the fuel mass will be used to develop a differential equation for the change in fuel-air equivalence ratio of the system. The energy conservation equation will be expanded to obtain a differential equation for the change in temperature of the thermodynamic system.

3.1 Conservation of Mass

3.1.1 Conservation of total mass

The rate of change of the total mass in any control volume or open system is equal to the sum of the mass flow rates into and out of the control volume, i.e.

$$\dot{m} = \sum_j \dot{m}_j \qquad (3\text{-}1)$$

Note that the convention used in our model assumes that mass flow rates into the control volume are taken as positive, while mass flow rates out of the control volume are negative.

3.1.2 Conservation of fuel mass

In particular, conservation of the fuel species can be expressed as

$$\dot{m}_f = \sum_j \dot{m}_{f,j} \qquad (3\text{-}2)$$

where m_f denotes the fuel content in the control volume (includes fuel added by injection and fuel in the form of combustion products).

Defining the fuel fraction, F, in the control volume as

$$F = m_f/m$$

where m is the total mass in the control volume, equation (3-2) can be re-written as

$$\frac{d}{dt}(mF) = \sum_j \dot{m}_j F_j \tag{3-3}$$

where F_j denotes the fuel fraction of the mass flow entering or leaving the control volume through the j port.

Differentiating the left-hand side of equation (3-3) gives

$$\dot{m}F = \sum_j \dot{m}_j F_j - \dot{m}F \tag{3-4}$$

or substituting for $\dot{m}$ from equation (3-1) results in a differential equation for the change in the fuel fraction of the control volume, i.e.

$$\dot{F} = \sum_j (\dot{m}_j/m)(F_j - F) \tag{3-5}$$

An average fuel-air equivalence ratio, ϕ, for the contents of the control volume can be defined as

$$\phi = \frac{m_f/m_a}{FASTO} \tag{3-6}$$

where m_a is the mass of air in the control volume and FASTO denotes the stoichiometric fuel to air ratio.

Expressing the equivalence ratio, ϕ, in terms of the fuel fraction, F, i.e.

$$\phi = \frac{1}{FASTO}\,\frac{F}{1-F} \tag{3-7}$$

and differentiating (3-7) with respect to time we obtain an equation for the rate of change of the equivalence ratio of the control volume, i.e.

$$\dot{\phi} = \frac{1}{\text{FASTO}} \frac{\dot{F}}{(1-F)^2} \tag{3-8}$$

with $\dot{F}$ given from equation (3-5).

3.2 Conservation of Energy

The general energy equation for an open thermodynamic system may be written as

$$\dot{E} = \sum_j \dot{m}_j h_j - \dot{Q}_w - \dot{W} \tag{3-9}$$

with the rate of change of the energy of the system being given by

$$\dot{E} = \frac{d}{dt}(mh) - \frac{d}{dt}(pV) \tag{3-10}$$

where

$\sum_j \dot{m}_j h_j$ is the net rate of influx of enthalpy

$\dot{Q}_w = \sum_i \dot{Q}_i$ is the total heat transfer to the walls, i.e. the sum of the heat transfer rates to the different surfaces of the control volume of interest

$\dot{W} = \dot{pV}$ is the rate at which the system does work by boundary displacement.

The dots denote differentiation with respect to time. Note that the convention used is that heat loss from the system and work done by the system are taken as positive.

Differentiating the left-hand side of equation (3-9) gives

$$\dot{m}\dot{h} = \sum_j \dot{m}_j h_j - \dot{Q}_w + \dot{p}V - \dot{m}h \qquad (3\text{-}11)$$

The contents of any control volume, i.e. air and combustion products, can be represented as one continuous medium by defining an average equivalence ratio at all times. Gas properties are obtained assuming ideal gas behavior and thermodynamic equilibrium. With these assumptions, we can express the enthalpy, h, and the density, ρ, of the mixture of air and combustion products as

$$h = h(T,p,\phi) \qquad (3\text{-}12)$$

$$\rho = \rho(T,p,\phi) \qquad (3\text{-}13)$$

Hence, the rate of change of the above fluid properties with respect to time, or crank-angle, can be written as

$$\dot{h} = c_p \dot{T} + c_T \dot{p} + c_\phi \dot{\phi} \qquad (3\text{-}14)$$

where

$$c_p = \left(\frac{\partial h}{\partial T}\right)_{p,\phi}$$

$$c_T = \left(\frac{\partial h}{\partial p}\right)_{T,\phi}$$

$$c_\phi = \left(\frac{\partial h}{\partial \phi}\right)_{T,p}$$

and

$$\dot{\rho} = \left(\frac{\partial \rho}{\partial T}\right)_{p,\phi} \dot{T} + \left(\frac{\partial \rho}{\partial p}\right)_{T,\phi} \dot{p} + \left(\frac{\partial \rho}{\partial \phi}\right)_{T,p} \dot{\phi} \qquad (3\text{-}15)$$

The equation of state for ideal gases

$$p = R\rho T \qquad (3\text{-}16)$$

can be expressed in differential form as

$$\frac{\dot{p}}{p} = \frac{\dot{R}}{R} + \frac{\dot{\rho}}{\rho} + \frac{\dot{T}}{T} \tag{3-17}$$

Re-arranging equation (3-17) and using (3-16), we can write

$$\dot{R} = \frac{1}{\rho T}\dot{p} - \frac{p}{\rho^2 T}\dot{\rho} - \frac{p}{\rho T^2}\dot{T} \tag{3-18}$$

Substituting for $\dot{\rho}$ from equation (3-15) into the above equation, we can express $\dot{R}$ in terms of $\dot{p}$, $\dot{T}$ and $\dot{\phi}$, i.e.

$$\dot{R} = \left(\frac{1}{\rho T} - \frac{p}{\rho^2 T}\frac{\partial \rho}{\partial p}\right)\dot{p} - \left(\frac{p}{\rho T^2} + \frac{p}{\rho^2 T}\frac{\partial \rho}{\partial T}\right)\dot{T} - \frac{p}{\rho^2 T}\frac{\partial \rho}{\partial \phi}\dot{\phi} \tag{3-19}$$

From the differential form of the equation of state, we can express the time rate of change of pressure as

$$\dot{p} = p\left(\frac{\dot{R}}{R} + \frac{\dot{m}}{m} + \frac{\dot{T}}{T} - \frac{\dot{V}}{V}\right) \tag{3-20}$$

or substituting for $\dot{R}$ from equation (3-19), and with some manipulation, we obtain the time rate of change of pressure:

$$\dot{p} = \frac{\rho}{\partial \rho / \partial p}\left(-\frac{\dot{V}}{V} - \frac{1}{\rho}\frac{\partial \rho}{\partial T}\dot{T} - \frac{1}{\rho}\frac{\partial \rho}{\partial \phi}\dot{\phi} + \frac{\dot{m}}{m}\right) \tag{3-21}$$

Returning to the energy equation (3-11), and expressing $\dot{h}$ in terms of its partial derivatives with respect to T, p and ϕ, we obtain

$$mc_P\dot{T} = \sum_j \dot{m}_j h_j - \dot{Q}_w + (V - mc_T)\dot{p} - mc_\phi\dot{\phi} - h\dot{m} \tag{3-22}$$

Finally, substituting for $\dot{p}$ from equation (3-21), we obtain an equation for the rate of change of temperature that does not explicitly depend on the rate of change of pressure of the system, i.e.

$$mc_p\dot{T} = (\Sigma_j \dot{m}_j h_j - \dot{Q}_w) - mc_\phi\dot{\phi} - h\dot{m} +$$

$$+ mB(-\frac{\dot{V}}{V} - \frac{1}{\rho}\frac{\partial\rho}{\partial T}\dot{T} - \frac{1}{\rho}\frac{\partial\rho}{\partial\phi}\dot{\phi} + \frac{\dot{m}}{m}) \qquad (3\text{-}23)$$

where $B = \frac{1}{(\partial\rho/\partial p)}(1 - \rho c_T)$ (3-24)

or dividing (3-23) by m, and collecting terms in $\dot{T}$, $\dot{\phi}$ and $\dot{m}$ get

$$(c_p + \frac{B}{\rho}\frac{\partial\rho}{\partial T})\dot{T} = \frac{1}{m}(\Sigma_j \dot{m}_j h_j - \dot{Q}_w) - (c_\phi + \frac{B}{\rho}\frac{\partial\rho}{\partial\phi})\dot{\phi} +$$

$$+ B\frac{\dot{m}}{m}(1 - \frac{h}{B}) - B\frac{\dot{V}}{V} \qquad (3\text{-}25)$$

leading to

$$\dot{T} = \frac{B}{A}[\frac{\dot{m}}{m}(1 - \frac{h}{B}) - \frac{\dot{V}}{V} - \frac{C}{B}\dot{\phi} + \frac{1}{Bm}(\Sigma_j \dot{m}_j h_j - \dot{Q}_w)] \qquad (3\text{-}26)$$

where

$$A = c_p + \frac{B}{\rho}\frac{\partial\rho}{\partial T} = c_p + \frac{(\partial\rho/\partial T)}{(\partial\rho/\partial p)}(\frac{1}{\rho} - c_T) \qquad (3\text{-}27)$$

$$C = c_\phi + \frac{B}{\rho}\frac{\partial\rho}{\partial\phi} = c_\phi + \frac{(\partial\rho/\partial\phi)}{(\partial\rho/\partial p)}(\frac{1}{\rho} - c_T) \qquad (3\text{-}28)$$

4. APPLICATION OF CONSERVATION EQUATIONS TO ENGINE PROCESSES

The conservation equations derived in section 3 can be applied to the four engine processes as follows:

i) Intake

$$\dot{m} = \dot{m}_{in} - \dot{m}_{ex} \tag{4-1}$$

$$\dot{F} = \frac{\dot{m}_{in}}{m}(F_{in} - F) - \frac{\dot{m}_{ex}}{m}(F_{ex} - F) \tag{4-2}$$

$$\dot{T} = \frac{B}{A}\left[\frac{\dot{m}}{m}\left(1 - \frac{h}{B}\right) - \frac{\dot{V}}{V} - \frac{C}{B}\dot{\phi} + \frac{1}{Bm}(\dot{m}_{in}h_{in} - \dot{m}_{ex}h_{ex} - \dot{Q}_w)\right] \tag{4-3}$$

ii) Compression

$$\dot{m} = 0 \tag{4-4}$$

$$\dot{F} = 0 \tag{4-5}$$

$$\dot{T} = \frac{B}{A}\left[-\frac{\dot{V}}{V} - \frac{\dot{Q}_w}{Bm}\right] \tag{4-6}$$

(iii) Combustion

$$\dot{m} = \dot{m}_f \tag{4-7}$$

$$\dot{F} = \frac{\dot{m}_f}{m}(1 - F) \tag{4-8}$$

$$\dot{T} = \frac{B}{A}\left[\frac{\dot{m}_f}{m}\left(1 - \frac{h}{b}\right) - \frac{\dot{V}}{V} - \frac{C}{B}\dot{\phi} + \frac{1}{BM}(\dot{m}_f h_f - \dot{Q}_w)\right] \tag{4-9}$$

where h_f is the absolute fuel enthalpy.

(iv) Exhaust

$$\dot{m} = -\dot{m}_{ex} \tag{4-10}$$

$$\dot{F} = -\frac{\dot{m}_{ex}}{m}(F_{ex} - F) \tag{4-11}$$

$$\dot{T} = \frac{B}{A}\left[-\frac{\dot{m}_{ex}}{m}\left(1 - \frac{h}{B}\right) - \frac{\dot{V}}{V} - \frac{C}{B}\dot{\phi} + \frac{1}{Bm}\left(-\dot{m}_{ex}h_{ex} - \dot{Q}_{w}\right)\right] \tag{4-12}$$

Note that the fuel fraction of the mass flow rate through the exhaust port, F_{ex}, could be different from the cylinder fuel fraction, F, in reverse flow situations.

5. MODELLING OF ENGINE PROCESSES

5.1 Gas Exchange

A one-dimensional quasi-steady compressible flow model is used to calculate the mass flow rates through the intake and the exhaust valves during the gas exchange process. The manifolds are treated as plenums with known pressures. Furthermore, the temperature and average equivalence ratio of the intake charge (fresh air and EGR at intake manifold conditions) and the exhaust charge (mixture of air and combustion products at cylinder conditions) are known. When reverse flow into the intake manifold occurs, a rapid-mixing model is used, i.e. perfect and instantaneous mixing between the back-flowing charge and the intake charge is assumed.

At each step of the gas exchange process, values for the valve open areas and discharge coefficients are obtained from tabulated data. Given the open area, the discharge coefficient, and the pressure ratio across a particular valve, the mass flow rate across that valve is calculated from:

$$\dot{m} = c_d A \frac{p_o}{RT_o}\sqrt{\gamma R T_o}\left\{\frac{2}{\gamma-1}\left[\left(\frac{p_s}{p_o}\right)^{2/\gamma} - \left(\frac{p_s}{p_o}\right)^{(\gamma+1)/\gamma}\right]\right\}^{1/2} \qquad (5\text{-}1)$$

where

c_d = discharge coefficient

A = valve open area

p_o = stagnation pressure upstream of restriction

p_s = static pressure at restriction

T_o = stagnation temperature upstream of restriction

γ = ratio of specific heats

R = gas constant

When the kinetic energy in the cylinder is negligible, the stagnation

pressure and temperature reduce to the static pressure and temperature, respectively.

For the case of choked flow, equation (5-1) reduces to

$$\dot{m} = c_d A \frac{p_o}{RT_o} \sqrt{\gamma RT_o} \left(\frac{2}{\gamma+1}\right)^{(\gamma+1)/2(\gamma-1)} \tag{5-2}$$

The mass, m(t), in the cylinder at any time t can be found from integration of the mass conservation equation (3-1), i.e.

$$m(t) = m_o + \int_{t_o}^{t} \dot{m}_{in}\,dt - \int_{t_o}^{t} \dot{m}_{ex}\,dt \tag{5-3}$$

where m_o is the mass in the cylinder at cycle start (IVO).

5.2 Combustion Model

The diesel combustion process is a very complex, unsteady, heterogeneous, three-dimensional process. A good mathematical combustion analysis would require accurate models of compressible viscous air motion, fuel spray penetration, droplet break-up and evaporation, air entrainment, combustion kinetics, turbulent diffusion and so on. The details of the combustion process would depend on the characteristics of the fuel, the design of the combustion chamber and the fuel injection system, and on the engine's operating conditions. Although an adequate conceptual understanding of diesel combustion has been developed to date, a comprehensive quantitative model of all the individual processes has not yet been proposed.

A relatively successful approach to the problem of combustion simulation has been to model combustion as a heat release process, as originally proposed by Lyn [7]. The rate of heat release (or, equivalently, the rate of fuel burning) can be defined as the rate at which the chemical energy of the fuel is released by combustion. Based on heat release analysis and high-speed

photography, Lyn has provided an excellent description of the different stages of diesel combustion. These stages can be identified on the typical rate of heat release diagram for a DI engine shown in Fig. 2 as follows:

Ignition delay (ab): The period between the dynamic injection point (the point at which the injector needle starts to lift) and the ignition point (the start of positive heat release due to combustion).

Pre-mixed or rapid combustion phase (bc): In this phase, combustion of the fuel which has mixed with air to within the flamability limits during the ignition delay period occurs rapidly in a few crank angle degrees. This results in the high initial rate of burning generally observed in direct-injection diesel engines.

Mixing controlled combustion phase (cd): Once the fuel and air premixed during the ignition delay have been consumed, the heat release rate (or burning rate) is controlled by the rate at which mixture becomes available for burning. The heat release rate may or may not reach a second (usually lower) peak in this phase; it decreases as this phase progresses.

Late combustion phase (de): Heat release continues at a low rate well into the expansion stroke. Eventually, the burning rate asymptotically approaches zero. The nature of combustion during this phase is not well understood. Possible processes are that a small fraction of the fuel may not yet have burned, or energy present in soot and fuel-rich combustion products can still be released, etc. Given the somewhat arbitrary limits of this phase, combustion models usually focus on the main heat release periods, i.e. the pre-mixed and mixing controlled combustion phases.

Based on his observations, Lyn [7] proposed a method of predicting burning rates from the rate of fuel injection. The fuel injected is divided into elements according to the order in which they enter the combustion chamber. These fuel elements become "ready for burning" according to a certain law (with increasing burning time as injection proceeds). Thus, a "ready for burning" diagram can be obtained from the rate of injection diagram. At the ignition point, which occurs after the lapse of the delay period, the part of the injected fuel which has been made "ready for burning" is added on the total "ready for burning" diagram, causing the sharp peak in the burning rate diagram. Subsequent burning is essentially proportional to the rate of injection. Although this method gives a reasonable fit to data obtained over a wide range of speeds and loads, it requires further refinement and calibration before it can be used in computer simulation work.

It is necessary in combustion modelling, in the context of computer simulation to predict the performance of new engine concepts, to describe the apparent fuel burning rate by algebraic expressions. The constants in these expressions can be chosen suitably to reflect the dependence of the actual fuel burning rate on engine type and particular operating conditions.

Shipinski et al [8] attempted to correlate the apparent rate of fuel burning with the rate of fuel injection by fitting a Wiebe function to heat release diagrams obtained from tests on a high-speed swirl-type direct injection engine. Although Shipinski obtained a reasonable agreement with his engine data, the heat release shape defined by the Wiebe function alone has a notable difference from the two-part characteristic with the initial spike that is measured on most engine types.

To overcome this problem, Watson et al [9] proposed that the apparent fuel burning rate could be expressed as the sum of two components, one relating to pre-mixed and the other to diffusion-controlled burning, i.e.

$$\dot{m}_t = \dot{m}_p + \dot{m}_d \qquad (5\text{-}4)$$

where $\dot{m}$ is the fuel burning rate with respect to crank angle

and subscripts t, p, d denote total, pre-mixed and diffusion burning, respectively.

In order to quantify the proportion of the fuel burnt by either mechanism, a phase proportionality factor, β, is introduced. This expresses the cumulative fuel burnt by pre-mixed burning as a fraction of the total fuel injected, i.e.

$$\beta = \frac{m_p}{m_t} \qquad (5\text{-}5)$$

Consequently, a non-dimensional apparent fuel burning rate curve can be written as

$$\dot{M}_t(\tau) = \beta \dot{M}_p(\tau) + (1 - \beta)\dot{M}_d(\tau) \qquad (5\text{-}6)$$

where $\dot{M}(\tau)$ = non-dimensional burning rate distribution

and τ = normalized crank position.

The phase proportionality factor, β, is considered to be controlled by the length of the ignition delay period (since the fuel that is prepared for burning during this period governs the pre-mixed burning phase), and the overall cylinder equivalence ratio, ϕ_{ove}. This can be expressed by a relation of the form

$$\beta = 1 - a\frac{\phi_{ove}^{\ b}}{ID^c} \qquad (5\text{-}7)$$

where ID = ignition delay (see Section 5.3).

From correlation with data from turbo-charged truck engines, Watson [9] obtained the following range of values for a, b, and c:

$$0.8 < a < 0.95$$
$$0.25 < b < 0.45 \qquad (5\text{-}8)$$
$$0.25 < c < 0.50$$

Futhermore, Watson concluded that the best representation of the experimental data was achieved using the following component burning rate distributions:

Premixed burning:

$$M_p(\tau) = 1 - (1 - \tau^{C_{p1}})^{C_{p2}} \qquad (5\text{-}9a)$$

or
$$\dot{M}_p(\tau) = C_{p1}C_{p2}\tau^{(C_{p1}-1)}(1 - \tau^{C_{p1}})^{(C_{p2}-1)} \qquad (5\text{-}9b)$$

Diffusion controlled burning (Wiebe function)

$$M_d(\tau) = 1 - \exp(-C_{d1}\tau^{C_{d2}}) \qquad (5\text{-}10a)$$

or
$$\dot{M}_d(\tau) = C_{d1}C_{d2}\tau^{(C_{d2}-1)}\exp(-C_{d1}\tau^{C_{d2}}) \qquad (5\text{-}10b)$$

where C_{p1}, C_{p2}, C_{d1}, C_{d2} are shape factors.

The shape factors in equations (5-9) and (5-10) can be determined as a function of the engine operating conditions. Using data from a typical truck engine, Watson established the following correlations:

$$C_{p1} = 2.0 + 1.25 \times 10^{-8}(ID \times N)^{2.4} \qquad (5\text{-}11a)$$

$$C_{p2} = 5000 \qquad (5\text{-}11b)$$

$$C_{d1} = 14.2\ \phi_{ove}^{-0.644} \qquad (5\text{-}11c)$$

$$C_{d2} = 0.79\, C_{d1}^{0.25} \qquad (5\text{-}11d)$$

where

ID = ignition delay (see Section 5.3)

N = engine speed (RPM)

ϕ_{ove} = overall cylinder equivalence ratio.

Watson's correlation gives good agreement between experimental and predicted results over the entire range of engine operating conditions, and is flexible enough to be applied to various types of diesel engines. Thus, we have followed Watson's approach to describe the heat release profile for our engine simulation. If necessary, the constants (or the form) of correlations (5-7) and (5-11) will be modified to fit experimental data for our engine design.

5.3 Ignition Delay Model

The ignition delay period in a diesel engine was defined in section 5.2 as the time (or crank angle) interval between the start of injection and the start of combustion. The start of injection is usually taken as the time when the injector needle lifts off its seat (determined from a needle lift indicator). The start of combustion is more difficult to determine. It is best identified from the change in slope of the heat release rate which occurs at ignition.

Both physical and chemical processes must take place before the injected fuel can burn. The physical processes are: the atomization of the liquid fuel jet; the vaporization of the fuel droplets; the mixing of fuel vapor with air. The chemical processes are the precombustion reactions of the fuel, air,

residual gas mixture which lead to autoignition. These processes are affected by engine design and operating variables, and fuel characteristics.

Ignition delay data from fundamental experiments in combustion bombs and flow reactors have usually been correlated by equations of the form

$$ID = A\, p^{-n} \exp(E/RT) \qquad (5\text{-}12)$$

where ID = ignition delay [ms]

E = apparent activation energy for the fuel autoignition process

R = universal gas constant

p = gas pressure [atm]

T = gas temperature [K]

and A and n are constants dependent on the fuel and the injection and air-flow characteristics. Representative values for A, n and E are given in Table 1.

These correlations have usually been derived from tests in uniform air environments where the pressure and temperature only changed due to the cooling effect of the fuel vaporization and fuel heating processes. However, in a diesel engine, pressure and temperature change considerably during the delay period due to the compression resulting from piston motion. Another problem is that the form of these simple correlations is not sufficiently flexible to allow all the influencing fuel and engine parameters to be included in the calculation of the ignition delay.

Hardenberg and Hase [10] have developed an empirical formula for predicting the ignition delay in DI engines as a function of fuel characteristics, engine parameters and ambient conditions. Dent [11] has shown that this formula can give reasonable agreement with experimental data over a wide range of engine conditions. However, the pressure and temperature

used in this correlation are identified as the corresponding conditions at top deal centre, estimated using a polytropic model for the compression process. It is felt that such a polytropic model is not appropriate in our simulation context, where pressures and temperatures can be accurately predicted over the duration of the ignition delay period. Therefore, we propose to use a formula similar to Equation (5-12), with pressure and temperature taken at their arithmetic mean values during the delay period to account for changing conditions.

5.4 Heat Transfer

The heat transfer mechanisms in a diesel engine include forced convection ($\dot{Q}_c$) from the turbulent flow in the cylinder to the combustion chamber walls, and radiation ($\dot{Q}_r$) from the flame and the burning soot particles. The total heat transfer rate ($\dot{Q}_w$) is therefore given by

$$\dot{Q}_w = \dot{Q}_c + \dot{Q}_r \qquad (5\text{-}13)$$

The convective heat transfer at the gas-to-cylinder wall interface will depend on the temperature gradient in the boundary layer at the surface. However, due to the inherent difficulties in calculating the boundary layers in a diesel engine, the convective heat transfer rate is usually expressed as

$$\dot{Q}_c = h\, A\, (T_g - T_w) \qquad (5\text{-}14)$$

where

h = convective heat transfer coefficient

A = surface area

T_g = bulk mean gas temperature

T_w = local surface temperature on cylinder wall, head, or piston, as appropriate.

The problem is then to devise a method to calculate the convective heat transfer coefficient that appears in (5-14). The approach usually taken is to calculate h from a Nusselt-Reynolds number correlation analagous to that used for steady turbulent flow in a pipe [12-16], i.e.

$$Nu = a\, Re^d\, Pr^e \tag{5-15}$$

where

$Nu = hL/\lambda$: Nusselt number

$Re = VL/\nu$: Reynolds number

$Pr = \mu c_p/\lambda$: Prandtl number

L = a characteristic length

V = a characteristic velocity

λ = thermal conductivity

ν = kinematic viscosity

μ = dynamic viscosity

ρ = density

c_p = specific heat at constant pressure

and a, d, e are constants adjusted to fit experimental data.

Fortunately, there is little variation in the Prandtl number for air and combustion products, which is usually close to unity. Consequently, we may drop the Prandtl number dependence in equation (5-15) with little loss in accuracy, so that

$$Nu = a\, Re^d \tag{5-16}$$

To calculate the convective heat transfer coefficient from correlation

(5-16), instantaneous values for the characteristic length and velocity scales, and the gas transport properties (μ, ρ, and λ) are needed. Currently, it is not possible to predict these parameters and their spatial and temporal variation with any accuracy in an internal combustion engine. To overcome this difficulty, representative values of the characteristic length and velocity scales, and the gas temperature, pressure, and equivalence ratio at which the gas properties are to be evaluated are chosen.

For our heat transfer model, the characteristic length scale is taken to be the macroscale of turbulence, as defined by equation (5-28). (See turbulent flow model). The characteristic velocity V is postulated to be an effective velocity due to contributions from the mean kinetic energy, the turbulent kinetic energy and piston motion, i.e.

$$V = [U^2 + u'^2 + (V_p/2)^2]^{1/2} \qquad (5\text{-}17)$$

where

U = mean flow velocity, defined by (5-20)

u' = turbulent intensity, defined by (5-21)

V_p = instantaneous piston speed

While this expression for V is speculative, it is constructed in such a way that increases in any of the three component velocities lead to increases in the heat transfer rate, while at the same time errors due to overestimating the contribution from any one component are minimized.

Many attempts have been reported to determine the constants a and d, either by experiments or trial and error. [12-16]. Suggested values are

$$a = 0.035 \text{ to } 0.13$$
$$d = 0.7 \text{ to } 0.8 \qquad (5\text{-}18)$$

depending on intensity of change motion. The gas density and the transport

properties, μ and λ, that appear in correlation (5-16) are evaluated at the mean gas temperature, pressure, and equivalence ratio.

Radiative heat flux is significant in diesel engines. However, due to the difficulty of measuring instantaneous flame temperature and heat flux, it is not easy to quantify the contribution of radiation to the overall heat transferred. Estimates of the relative importance of radiation have varied between a few and 30 percent of total heat transfer, and vary according to engine type. [13,14,17,18].

Annand [13] has expressed the radiation term as

$$\dot{Q}_r = k_r(T_g^4 - T_w^4) \qquad (5\text{-}19)$$

where

k_r = empirical radiation constant

T_g = bulk mean gas temperature

T_w = local surface temperature on cylinder wall, head or piston, as appropriate

During the intake, compression and exhaust processes, when the radiative heat flux would be zero, $k_r = 0$. During combustion, Annand and Ma [14] suggested that

$$k_r = C_r \sigma$$

where σ = Stephan-Boltzmann constant (56.7×10^{-12} kw/m^{2}K^4),

and C_r is an adjustable constant with values in the range of 1.3 - 3.1, depending on the engine speed and load. The value of C_r, exceeding unity, suggests that the actual radiation temperature is appreciably above the bulk mean value.

Spatial variations in heat transfer rates are accounted for by assigning different surface temperatures to the cylinder walls, head, piston, etc.,

based on practical experience. If these temperatures are to be calculated, a heat conduction model is required for the piston, valves, cylinder head, and liner.

The total instantaneous heat tranfer rate will be calculated from the sum of the convective terms (predicted by equation 5-14) plus the sum of the radiative terms (predicted by equation 5-19).

5.5 Turbulent Flow Model

The heat transfer model of the cycle simulation requires estimates of the characteristic velocity and length scales. To estimate these scales in a way which incorporates the key physical mechanisms affecting charge motion in the cylinder, a turbulent flow model is used. This model is a variation of the models used by Manscuri [5] and Poulos [4] in previous engine simulation work.

The turbulence model consists of a zero-dimensional energy cascade. Mean flow kinetic energy, K, is supplied to the cylinder through the valves. Mean kinetic energy, K is converted to turbulent kinetic energy, k, through a turbulent dissipation process. Turbulent kinetic energy is converted to heat through viscous dissipation. When mass flows out of the cylinder, it carries with it both mean and turbulent kinetic energy. Figure 3 illustrates the energy cascade model.

At any time during the cycle, the mean flow velocity, U, and the turbulent intensity, u', are found from knowledge of the mean and turbulent kinetic energies, K and k, respectively. Thus, the following equations apply:

$$K = \frac{1}{2} m U^2 \qquad (5\text{-}20)$$

$$k = \frac{3}{2} m u'^2 \qquad (5\text{-}21)$$

where the factor 3 in equation (5-21) comes from assuming that the small scale turbulence is isotropic (and accounting for all three orthogonal fluctuating velocity components).

The time rate of change of the mean kinetic energy, K is given by

$$\frac{dK}{dt} = \frac{1}{2}\dot{m}_i V_i^2 - P - K\frac{\dot{m}_e}{m} \tag{5-22}$$

Similarly, the rate of change of the turbulent kinetic energy, k, is

$$\frac{dk}{dt} = P - m\varepsilon - k\frac{\dot{m}_e}{m} + A \tag{5-23}$$

with $$\varepsilon = \frac{u'^3}{\ell} = \frac{(2k/3m)^{3/2}}{\ell} \tag{5-24}$$

where m = mass in the cylinder

$\dot{m}_i$ = mass flow rate into the cylinder

$\dot{m}_e$ = mass flow rate out of the cylinder

V_i = jet velocity into the cylinder

P = rate of turbulent kinetic energy production

ε = rate of turbulent kinetic energy dissipation per unit mass

A = rate of turbulent kinetic energy amplification due to rapid distortion

ℓ = characteristic size of large-scale eddies

In equations (5-22) and (5-23), the production term P has to be defined in terms of flow and geometrical parameters of the chamber. However, since the above model does not predict spatially resolved flow parameters, P must be estimated from mean flow quantities only.

Assuming that turbulence production in the engine cylinder is similar to turbulence production in a boundary layer over a flat plate [19], we can express P as

$$P = \mu_t \left(\frac{\partial U}{\partial y}\right)^2 \tag{5-25}$$

where $\mu_t = C_\mu k^2/(m\varepsilon)$ is turbulent viscosity,

and $C_\mu = 0.09$ is a universal constant.

Again, as the velocity field in the cylinder is not known, the velocity gradient $(\partial U/\partial y)$ is approximated as

$$\left(\frac{\partial U}{\partial y}\right)^2 = C_\beta \left(\frac{U}{L}\right)^2 \tag{5-26}$$

where C_β is an adjustable constant and L is a geometric length scale.

Using equations (5-25), (5-26), (5-20) and (5-24), we can express P as

$$P = 2\left(\frac{3}{2}\right)^{3/2} C_\mu C_\beta \left(\frac{K\ell}{L^2}\right)\left(\frac{k}{m}\right)^{1/2} \tag{5-27}$$

Furthermore, the characteristic size of the large-scale eddies, ℓ, and the representative geometric length scale, L will be both identified with the macroscale of turbulence, assumed to be given by

$$\ell = L = V/(\pi B^2/4) \tag{5-28a}$$

where V is the instantaneous volume of the combustion chamber and B is the cylinder bore, subject to the restriction that

$$L \leq B/2 \tag{5-28b}$$

Hence, equation (5-27) can be re-written as

$$P = 0.3307\ C_{\beta}\left(\frac{K}{L}\right)\left(\frac{k}{m}\right)^{1/2} \qquad (5\text{-}29)$$

During the compression and the combustion processes, the turbulent kinetic energy decays due to viscous dissipation. On the other hand, at the same time the turbulent kinetic energy is amplified due to the rapid distortion that the cylinder charge undergoes with rising cylinder pressures. Consequently, an amplification term, A, was added to equation (5-23) to account for this effect. The amplification term will be larger during combustion when the unburned gas is assumed to be compressed by the flame at a sufficiently high rate. However, in the diesel engine context (high compression ratios), it is proposed to keep the amplification term during compresson, too.

Using equation (5-21), the rate of turbulence amplification due to rapid distortion can be expressed as

$$A = 3\ m\ u'\ \frac{du'}{dt} \qquad (5\text{-}30)$$

where the rate of change of the turbulent intensity du'/dt can be estimated assuming that conservation of mass and angular momentum can be applied to the large scale eddies during the rapid distortion period.

Under these assumptions, conservation of mass for a single eddy of volume V_L requires that

$$\rho\ V_L = \rho_o\ V_{Lo} \qquad (5\text{-}31)$$

where ρ is the mean gas density and subscript o refers to the conditions at the start of compression. Then, since

$$V_L \sim L^3 \qquad (5\text{-}32)$$

where L is the macroscale of turbulence, we can re-write (5-31) as

$$\frac{L}{L_o} = \left(\frac{\rho_o}{\rho}\right)^{1/3} \tag{5-33}$$

Conservation of eddy angular momentum requires that

$$U_\omega L = U_{\omega o} L_o \tag{5-34}$$

where U_ω is the characteristic velocity due to eddy vorticity.

Combining (5-33) and (5-34) with the assumption that

$$U_\omega \sim u' \tag{5-35}$$

the following relation is obtained for the evolution of the turbulent intensity during the rapid compression period

$$\frac{u'}{u'_o} = \left(\frac{\rho}{\rho_o}\right)^{1/3} \tag{5-36}$$

Differentiating both sides of equation (5-36) and re-arranging we get

$$\frac{du'}{dt} = \frac{u'}{3\rho}\frac{d\rho}{dt} \tag{5-37}$$

Hence, combining equations (5-30) and (5-37), the rate of turbulence amplification is given by

$$A = \frac{mu'^2}{\rho}\frac{d\rho}{dt} \tag{5-38}$$

or, introducing (5-21),

$$A = \frac{2}{3} k \frac{\dot{\rho}}{\rho} \tag{5-39}$$

with $\dot{\rho}$ given from equation (3-15).

5.6 Engine Friction Model

To convert indicated engine performance quantities to brake engine performance quantities, engine friction calculations are required. However, the measurement and analysis of engine frictional losses has never been satisfactorily resolved. This is primarily due to the inherent problem of direct, accurate measurement of these losses under actual running conditions. This problem occurs because the total loss is a summation of losses arising from the operation of the many components of the engine, and these components respond differently to changes in pressure, temperature and speed.

Direct motoring of an engine is the common method of measuring losses, but clearly the motoring losses are not the same as the losses under firing conditions. Some of the reasons are the lower pressure acting on piston rings and bearings, the lower temperatures of the piston and cylinder bore surfaces and thus the greater oil viscosity, the greater running clearance of the piston, and the missing exhaust blowdown period.

Nevertheless, a breakdown analysis of motoring losses supplemented by experiments on piston and ring friction rigs can be used to identify the relative importance of the many components of the total friction and their response to changes in desigh variables. In general, the components of the losses expressed in terms of mep tend to fall into three groups:

(i) Losses due to boundary lubrication, approximately invariable with speed. There losses are undoubtedly influenced by the compression ratio.

(ii) Losses associated with oil film friction, varying directly as speed. All major rotating parts fall into this group.

(iii) Losses associated with air pumping, varying as the square of the speed.

Therefore, the motoring losses can be expressed in the form

$$F = A + BN + CN^2 \tag{5-39}$$

where F are the losses in mep, N is engine speed, and A, B and C are constants.

Millington and Hartles [20] have measured motoring losses on a large variety of automotive diesel engines during the course of development of prototype engines. Their work suggests a readjustment of equation (5-39) coupled with suitable selection of the constants as follows:

$$F = A + 7.0 \frac{N}{1000} + 1.5 \left(\frac{V}{1000}\right)^2 \tag{5-40}$$

where F = motoring losses, psi mep

A = compression ratio minus 4 for a DI diesel

N = engine speed, rpm

V = mean piston speed, fpm

Equation (5-40) represents a sound empirical correlation of the motoring loss data obtained from diesel engines. Therefore, it will be used to obtain brake quantities from the indicated quantities computed in the engine simulation.

6. BASIC ASSUMPTIONS OF OTHER COMPONENT MODELS

The configuration of the turbocharged, turbocompounded, Diesel system was shown in Fig.1. It consists of a compressor, intercooler, intake manifold, intake ports to the engine, multicylinder engine, exhaust ports, exhaust manifold, wastegate, turbocharger turbine, compounded turbine and associated ducting. The following simplifying assumptions were made in order to develop models of the components required in addition to the diesel engine to complete the overall system.

1. The intake air is at atmospheric conditions:

   $p_1 = p_{atm}$ and $T_1 = T_{atm}$

2. The compressor, turbine and power turbine are adiabatic; i.e. there is no heat transfer from these conponents to the environment.
3. There are no mass transfers except along the routes indicated; i.e. no loss or leakage from the system.
4. Intake air and exhaust gas can be modelled as ideal gases.
5. The connecting pipes to and from the manifolds can be included as parts of their respective manifolds, for modelling purposes.
6. There is perfect and instantaneous mixing of all mass flows that enter each manifold with the gases in the manifold, thus there is no variation in properties within a manifold at any instant of time, and all flows leaving a manifold have the properties of the manifold contents.
7. The wastegate bleeds off a fraction of the exhaust gas stream ($\dot{m}_w$), such that the flow bypasses the turbocharger turbine but not the power turbine.
8. The wastegate valve behaves as a throttle valve of variable effective throat area. The size of the opening can be governed by the intake manifold pressure, p_5.

9. The EGR flow is either specified as a fraction of the intake flow, or the EGR valve is modelled as a throttle valve of fixed effective throat area.
10. The flows through the wastegate and EGR valves are subsonic and adiabatic, and the throat pressures are equal to the downstream pressures.
11. The two exhaust gas streams, through and by-passing the turbine, ($\dot{m}_t$ and $\dot{m}_w$) reunite with no loss of thermal energy or pressure.
12. The inside wall temperature of all components in the system are known.
13. There are pressure drops between the following:
    compressor discharge and intercooler inlet (p_2 & p_3)
    intercooler inlet and intake manifold (p_3 & p_5)
    exhaust manifold and turbine inlet (p_7 & p_8)
    turbine discharge and power turbine inlet (p_9 & p_{10})
    power turbine discharge and atmosphere (p_{11} & p_{atm})
14. Wastegate upstream pressure equals turbine inlet pressure.
15. Wastegate downstream pressure equals turbine discharge pressure.
16. Turbine and compressor speeds are equal.
17. The turbocharger (turbine, compressor and shaft) has fixed values of rotational inertia and damping, relative to its housing (J and B, respectively).
18. The power turbine shaft is connected to the engine crankshaft via a specified gear ratio transmission, thus the power turbine speed is always determined directly from the engine speed.

7. MODELLING OF SYSTEM COMPONENTS

7.1 State Variables

The turbocharged diesel engine system described in Sec. 6 can be modelled mathematically by a set of simultaneous, non-linear differential equations involving a minimum set of dependent variables. These variables, called the state variables, are sufficient to describe completely the system at any point in time. Although their number is fixed by the system, there are many choices of state variables, some more convenient than others. The mass, temperature, absolute pressure and fuel fraction states of each manifold and the turbocharger speed were chosen as the nine state variables of this system. Crank-angle was chosen as the independent variable, rather than time. Since we are studying constant speed performance, time and crank-angle are directly proportional. All mass flow rates (m) in the following analysis refer to mass flow per unit crank angle.

7.2 Derivation of Differential Equations

7.2.1 Manifolds

The four state equations for each manifold are derived from four interdependent relations for the manifold control volume:

1. conservation of total mass
2. conservation of fuel mass
3. conservation of energy (first law of thermodynamics)
4. ideal gas law

The general manifold control volume model is shown in Fig. 4. The total mass and fuel fraction state equations for the manifold come directly from the continuity relations derived earlier (Equations (3-1) and (3-5), respectively):

$$\left(\frac{dm}{dt}\right)_m = \sum_j \dot{m}_j \tag{7-1}$$

$$\left(\frac{dF}{dt}\right)_m = \sum_j \frac{\dot{m}_j}{m_m} (F_i - F_m) \tag{7-2}$$

where the subscript m refers to the manifold control volume, and the subscript j refers to the j-th mass flow that enters or leaves the control volume.

For the intake manifold, the mass flows entering and leaving the manifold include:

i) compressor mass flow ($\dot{m}_c$ in Fig.1) (entering) which is found from the compressor map

ii) engine intake mass flow ($\dot{m}_{in}$ in Fig. 1) (leaving) which is found from the engine model

iii) EGR mass flow ($\dot{m}_{EGR}$ in Fig. 1) (entering) which is found from the EGR valve equations

For the exhaust manifold, the mass flows entering and leaving the manifold include:

i) turbine mass flow ($\dot{m}_t$ in Fig.1) (leaving) which is found from the turbine map

ii) engine exhaust mass flow ($\dot{m}_{ex}$ in Fig. 1) (entering) which is found from the engine model

iii) EGR mass flow ($-\dot{m}_{EGR}$ in Fig. 1) (leaving) which has the opposite sign to intake EGR flow)

iv) wastegate mass flow ($\dot{m}_w$ in Fig. 1) (leaving) which is found from the wastegate valve model

The state equation for temperature is derived from the general temperature state equation (3-26) applied to the manifold control volume.

$$\left(\frac{dT}{dt}\right)_m = \frac{1}{A}\left[\left(\frac{dm}{dt}_m\right)\frac{(B - h_m)}{m_m} - C\left(\frac{d\phi}{dt}_m\right) + \frac{1}{m_m}\left(\Sigma\, \dot{m}_j h_j - \dot{Q}\right)\right] \qquad (7\text{-}3)$$

where A, B, and C are defined in (3-27), (3-24), (3-28) and are calculated by the thermodynamic property subroutine,

$\dot{Q}$ = heat transfer rate to the manifold walls

and $d\phi/dt$ is related to dF/dt and F by (3-8).

The state equation for pressure is derived from the general pressure state equation applied to the manifold control volume (Eq. 3-21):

$$\left(\frac{dp}{dt}\right)_m = \frac{\rho}{\partial\rho/\partial p}\left[-\frac{1}{\rho}\frac{\partial\rho}{\partial T}\left(\frac{dT}{dt}_m\right) + \frac{1}{m}\left(\frac{dm}{dt}_m\right) - \frac{1}{\rho}\frac{\partial\rho}{\partial\phi}\left(\frac{d\phi}{dt}_m\right)\right] \qquad (7\text{-}4)$$

The mass, fuel fraction and temperature derivatives are calculated in equations (7-1), (7-2), and (7-3); the equivalence ratio derivative, $d\phi/dt$, is related to the fuel fraction derivative by Eq. (3-8); and the density derivatives are calculated by the thermodynamic property subroutine.

7.2.2 Turbocharger

The state equation describing the turbocharger is derived from the conservation of energy relation.

$$\frac{d}{dt}(E_{t/c}) = \dot{W}_{compressor} + \dot{W}_{turbine} \qquad (7\text{-}5)$$

where $$\frac{d}{dt}(E_{t/c}) = Jw\frac{d\omega}{dt} + B\omega^2 \qquad (7\text{-}6)$$

$E_{t/c}$ = total mechanical energy of turbocharger rotor

J = rotational inertia of turbocharger

B = rotational damping of turbocharger

ω = angular velocity

$$\dot{W}_{compressor} = \dot{m}_c(h_1 - h_2) \tag{7-7}$$

$$\dot{W}_{turbine} = \dot{m}_t(h_8 - h_9) \tag{7-8}$$

Solving for $d\omega/dt$ gives:

$$\frac{d\omega}{dt} = \frac{1}{J\omega}\{(\dot{m}_c(h_1 - h_2) + \dot{m}_t(h_8 - h_9) - B\omega^2\} \tag{7-9}$$

The enthalpy changes across the compressor and turbine are calculated using the compressible flow relations.

$$(h_1 - h_2) = -\frac{h_1}{\eta_c}\left[\left(\frac{p_2}{p_1}\right)^{R/c_p} - 1\right] \tag{7-10}$$

$$(h_8 - h_9) = \eta_t h_8\left[\left(\frac{p_8}{p_9}\right)^{R/c_p} - 1\right] \tag{7-11}$$

The complete state equation for turbocharger is found by combining equations (7-9), (7-10), and (7-11).

7.3 Wastegate and EGR Valve Models

The wastegate and exhaust gas recirculation (EGR) valves are modelled as adiabatic throttle valves of known effective throat area (which is the product of actual cross-sectional area and a discharge coefficient. The mass flow rates through the valves are calculated using (5-1) and (5-2).

To determine the EGR flow rate, either the percentage of the engine inlet flow which is EGR is specified, or the EGR valve opening is treated as a fixed effective-area orifice.

The wastegate valve opening area varies between zero and a fixed maximum value, $(C_D A)_{max}$, and is determined by an actuator linked to a pressure sensor. The sensor measures the gage pressure of the intake manifold. At present, a simple actuation model has been adopted which gives a continuous closed-form relation between effective valve throat area and intake manifold pressure. This model can be replaced when the actual actuator characteristics are available.

7.4 Intercooler Model

The intercooler, which is situated between the compressor discharge and intake manifold, serves to increase the density of the charge air by lowering its temperature. The intercooler is modelled as a heat exchanger of fixed area, heat-tranfer coefficient and cooling flow rate. The change in charge air temperature is determined from the non-dimensional heat exchanger effectiveness, ε.

$$\varepsilon = \frac{(T_{h1} - T_{h2})}{(T_{h1} - T_{c1})} \qquad (7\text{-}12)$$

where h refers to the charge air flow (hot)

c refers to the coolant flow (cold)

1 and 2 refer to inlet and exit conditions respectively

T_{h1} = compressor discharge temperature, T_2

T_{h2} = intercooler discharge temperature, T_4

T_{c1} = coolant inlet temperature (assumed to be fixed)

Heat exchanger effectiveness is either known as a design parameter or can be derived from graphical correlations that are available for the various typical heat exchanger configurations. From the latter ε can be determined as

a function of capacity rate ratio, C_{min}/C_{max}, and number of heat transfer units, N_A, where

C_{min} = the lesser of the two values of mc_p (assumed to belong to the charge air flow),

C_{max} = the greater of the two values of mc_p (assumed to belong to the coolant flow and to be fixed),

$N_A = AU/C_{min}$

A = heat exchange surface area (fixed)

U = heat transfer coefficient based on A

Fig. 5 shows a graphical correlation for a cross-flow heat-exchanger with unmixed flows, with various ratios of C_{min}/C_{max}. Currently the assumption is being made that C_{max} is much larger than C_{min}. With this assumption the expression for effectiveness reduces to the following simple form:

$$\varepsilon = 1 - \exp(-N_A) \qquad (7\text{-}13)$$

7.5 Manifold Heat Transfer

With the incorporation of an intercooler, heat transfer from the intake manifold to the environment becomes small enough to be neglected. Heat transfer from the exhaust manifold, however, cannot be neglected. Heat transfer from the gas in the exhaust manifold to the environment involves a combination of forced convective heat transfer from the gas to the inside walls, conduction from the inside walls to the outside walls and to the water jacket, and natural (and probably forced) convection from the outer surfaces to the environment.

It is clearly a complicated process to determine fully the heat transfer from inside gas to outside air, involving many detailed assumptions about engine geometry and environmental flow conditions. To simplify this task in

the current generation simulation program we will deal only with the modelling of the heat transfer from manifold gas to interior walls, which necessitates that a value for the wall temperature be assumed.

The heat transfer coefficient is derived from an experimental correlation that relates Nusselt, Reynolds and Prandtl numbers for fully-developed turbulent flow in circular tubes with large temperature gradients (Eq. 7-14).

$$Nu = \frac{UD}{k_b} = 0.035 \left(\frac{VD\rho_f}{\mu_f}\right)^{0.8} \left(\frac{c_p \mu}{k}\right)_b^{0.4} \qquad (7\text{-}14)$$

where D = exhaust manifold diameter

V = average velocity of gas

The gas properties are:

k = thermal conductivity

μ = absolute viscosity

ρ = density

c_p = specific heat at constant pressure

Subscripts are:

b: refers to properties at T_b.

f: refers to properties at T_f.

Temperatures are:

T_b = bulk (average) temperature

T_w = wall temperature

T_f = "film" temperature,

$$T_f = \frac{1}{2}(T_w + T_b) \qquad (7\text{-}15)$$

7.6 Pressure Losses

Pressure loss terms have been included at five locations in the overall system model. These are:

between compressor discharge and intercooler inlet,

across intercooler,

between exhaust manifold and turbine inlet,

between turbine outlet and power turbine inlet

between power turbine outlet and atmosphere.

Each of these pressure drops is calculated using the corresponding friction factors and friction coefficients for the geometry of each passage.

For straight-sections:

$$P = 4f(L/D)(\rho V^2/2) \tag{7-16}$$

where L = length of passage

D = diameter of passage

ρ = bulk density

V = average velocity

f = friction factor, which is correlated by (7-17) for the surface roughness and range of Reynolds numbers to be encountered.

Note that

$$f = 0.046(Re)^{0.2} \tag{7-17}$$

with $Re = \rho VD/\mu$

For bends, enlargements, contractions, etc:

$$P = K_f \rho V^2/2 \tag{7-18}$$

where K_f = friction coefficient for a particular passage geometry. Values of K_f for typical geometries are commonly available.

8. THERMODYNAMIC PROPERTIES

Our thermodynamic model assumes that the various control volumes contain mixtures of air and combustion products throughout the total engine system. By utilizing the concept of the instantaneous average equivalence ratio defined in Section 3.1, the contents of any control volume can be represented as one continuous medium. Furthermore, assuming ideal gas behavior and thermodynamic equilibrium, the instantaneous gas properties can be determined from a knowledge of pressure, temperature and average equivalence ratio in the control volume.

When the temperature of the cylinder contents is below 1000 K, they are treated as a homogeneous mixture of non-reacting ideal gases, their properties being calculated using the procedure outlined below [21]:

The hydrocarbon-air combustion reaction is written as:

$$\varepsilon\phi\ CH_y + O + \psi N \rightarrow x_1 CO + x_2 H_2O + x_3 CO + x_4 H_2 + x_5 O_2 + \psi N \qquad (8\text{-}1)$$

where ψ = the molar N:O ratio of the products,

y = the molar H:C ratio of the fuel,

ϕ = the average equivalence ratio,

x_i = moles of species i per mole of O_2 reactant

and $\varepsilon = 4/(4+y)$ (8-2)

The quantities x_i are determined by using the following assumptions:

a) for lean mixtures ($\phi \leq 1$) H_2 can be neglected.

b) for rich mixtures ($\phi > 1$) O_2 can be neglected.

c) for rich mixtures, the gas water reaction

$$CO_2 + H_2 \rightarrow CO_2 + H_2O$$

is in equilibrium with equilibrium constant K(T).

The solution for the x_i is shown in Table II, where C is obtained by solving equation (8-3) for its positive root.

$$(1 - K)C^2 + 2[1 - \varepsilon\phi + K(\phi - 1 + \varepsilon\phi)]C - 2K\varepsilon\phi(\phi - 1) = 0 \qquad (8\text{-}3)$$

The value of K(T) is obtained by curve fitting JANAF table data over the temperature range 400 to 3200 K and is given by

$$\ln(K(T)) = 2.743 - 1.761/t - 1.611/t^2 + .2803/t^3 \qquad (8\text{-}4)$$

where t = T/1000, and T is the temperature in Kelvins.

If the grams of products per mole of O_2 reactant is expressed as

$$M = (8\varepsilon + 4)\phi + 32 + 28\psi \qquad (8\text{-}5)$$

the specific enthalpy h and the specific heats at constant pressure and constant composition, c_p and c_ϕ respectively, can be expressed by the following relationships:

$$h = \frac{1}{M} \sum_{i=1}^{6} x_i \sum_{j=1}^{4} \left(a_{ij} \frac{t^j}{j} - \frac{a_{i5}}{t} + a_{i6}\right) \qquad (8\text{-}6)$$

$$c_p = \frac{1}{M} \sum_{i=1}^{6} x_i \sum_{j=1}^{4} \left(a_{ij} t^{j-1} + \frac{a_{i5}}{t^2}\right) \qquad (8\text{-}7)$$

$$c_\phi = \frac{1}{M} \sum_{i=1}^{6} \frac{\partial x_i}{\partial \phi} \sum_{j=1}^{4} \left(a_{ij} \frac{t^j}{j} - \frac{a_{i5}}{t} + a_{i6}\right) -$$

$$- \frac{\partial M/\partial \phi}{M^2} \sum_{i=1}^{6} x_i \sum_{j=1}^{4} \left(a_{ij} \frac{t^j}{j} - \frac{a_{i5}}{t} + a_{i6}\right) \qquad (8\text{-}8)$$

The coefficients a_{ij} are obtained by curve fitting JANAF table data to the above functional form. The values of a_{ij} are given in Table III. The resultant c_p is in cal/g-K, while h and c_ϕ are in kcal/g.

Since the cylinder contents are being treated as a mixture of non-reacting ideal gases, the density of the mixture is given by

$$\rho = \frac{p\bar{M}}{R_o T} \tag{8-9}$$

where

R_o = the universal gas constant (1.9869 cal/mole-K)

and $\bar{M}$, the average molecular weight of the mixture, is given by

$$M/((1 - \varepsilon)\phi + 1 + \psi) \qquad \phi \leq 1$$

and (8-10)

$$M/((2 - \varepsilon)\phi + \psi) \qquad \phi > 1$$

Then, the partial derivatives of the density with respect to temperature, pressure, and equivalence ratio are given by

$$\frac{\partial \rho}{\partial T} = -\frac{\rho}{T} \tag{8-11}$$

$$\frac{\partial \rho}{\partial p} = \frac{\rho}{p} \tag{8-12}$$

$$\frac{\partial \rho}{\partial \phi} = \frac{\partial \rho}{\partial \bar{M}} \frac{\partial \bar{M}}{\partial \phi} = \frac{\rho}{\bar{M}} \frac{\partial \bar{M}}{\partial \phi} \tag{8-13}$$

When the temperature of the cylinder contents is above 1000 K, their properties are calculated with allowance for chemical dissociation, according to the calculation method described in [22]. This is an approximate method based on curve fitting data obtained from detailed thermochemical calculations [23] to a functional form obtained from concentrations within the burned gases are not calculated, the bulk thermodynamic properties needed for cycle analysis are accurately determined.

9. TRANSPORT PROPERTIES

The heat transfer correlations relate the heat transfer coefficient to the Reynolds and Prandtl numbers and the thermal conductivity. The calculation of the heat transfer rates will therefore require values for the viscosity and the Prandtl number (from which the thermal conductivity can be obtained). We have used the approximate correlations for the viscosity and the Prandtl number of hydrocarbon-air combustion products developed by Mansouri and Heywood [24].

The NASA equilibrium program [23] was used to compute the viscosity of hydrocarbon-air combustion products as a function of temperature, T, equivalence ratio, ϕ, and pressure p. It was shown that the viscosity of the combustion products was satisfactorily correlated by a power-law based on air viscosity data, corrected for the effect of equivalence ratio, i.e.,

$$\mu_{prod}\ [kg/ms] = 3.3\times10^{-7}T^{0.7}/(1 + 0.027\phi) \qquad (9\text{-}1)$$

for $500\ K \leq T \leq 4000\ K$

$0 \leq \phi \leq 4$

Note that the viscosity of the combustion products is independent of the pressure.

The equilibrium Prandtl number of hydrocarbon-air combustion products was also calculated over the above ranges of temperature, pressure, and equivalence ratio. Using a second order polynomial of γ to curve fit the above data, it was shown that the following correlation for lean ($\phi < 1$) mixtures predicted values in good agreement (within 5%) with the data, i.e.,

$$Pr = 0.05 + 4.2(\gamma - 1) - 6.7(\gamma - 1)^2 \qquad (9\text{-}2a)$$

for $500\ K \leq T \leq 4000\ K$

and $\phi \leq 1$

For rich mixtures ($\phi > 1$), a reasonable fit (less than 10% error) to the equilibrium Prandtl number values calculated with the NASA program was found to be the following:

$$Pr = [0.05 + 4.2(\gamma - 1) - 6.7(\gamma - 1)^2]/[1 + 0.015 \times 10^{-6}(\phi T)^2] \qquad (9\text{-}2b)$$

for $2000\ K \leq T \leq 3500\ K$

and $1 < \phi \leq 4$

10. ITERATION PROCEDURE

10.1 Basic Method of Solution

When the individual submodels of the total engine system are brought together to form a complete model, the result is a set of simultaneous first-order ordinary differential-equations. To perform predictive calculations with the cycle simulation, these equations must be integrated simultaneously over the full operating cycle. Note, however, that some of the governing equations like the mass flow rate through the intake or the exhaust valve and the non-dimensional fuel burning rate apply only during parts of the cycle.

Integration of the governing equations is performed numerically using a standardized code developed by Shampine and Gordon [27]. The optimal integration time step is calculated automatically in the routine so as to maximize efficiency. Detailed documentation of the integration routine is provided in the listing of the code.

10.2 Crank Angle By Crank Angle Integration

The engine model calculates the state variables in one master cylinder of a multi-cylinder engine, while the manifold and other component models have inherent multi-cylinder capability. The interaction between the master cylinder model and the other components takes place in the manifolds. To simulate the effect of additional cylinders on the manifold conditions and hence on the entire system behavior, the conditions in the other cylinders are assumed to vary as echoes of the first cylinder, shifted by the appropriate phase lags. The intake and exhaust mass flow profiles calculated by the engine model for the master cylinder are used to represent the profiles for the other cylinders. These profiles are updated after the completion of each engine cycle for use in the next iteration.

A flow chart showing the overall structure of the engine cycle simulation is shown in Figure 6. After the initialization of the state variables, the simulation proceeds with the simultaneous integration of the state equations for the manifolds, the engine and the turbocharger. The main program determines which sets of equations the integrator will work with, and calculates and prints our results as the cycle proceeds. Four secondary routines corresponding to the intake, compressor, combustion, and exhaust processes are called in turn by the integration routine to supply it with the derivatives of the variables which it must integrate. A third level of utility routines, such as the other component state equations, thermodynamic and transport property routines, tables of valve flow areas and discharge coefficients, is called by the second level routines to help in the evaluation of the necessary derivatives at each step.

Approximate estimates of all state variables at convergence are assumed. In general, more than one iteration is required to model an engine operation under steady conditions. The integration continues until the system reaches a quasi-steady state, which is defined as the state in which the value of each state variable at a particular crank-angle is the same (to within a specified interval) as it was at that crank-angle in the previous engine cycle. Thus, at quasi-steady state a set of repeating patterns of variation, one for each state in the system and each with a period of one engine revolution, is achieved.

11. PROGRAM INPUTS AND OUTPUTS

11.1 Inputs

To operate the simulation, a set of input parameters must be specified. These include fixed system dimensions, initial values of state variables and computing tolerances. They are listed and briefly described below.

11.1.1 Engine operating conditions

i. fuel type

ii. mass of fuel injected per cycle

iii. injection timing

iv. engine speed (rpm)

v. constants in the ignition delay correlation

vi. nominal burning duration

vii. constants related to the burning rate distributions

11.1.2 System dimensions and design parameters

a. Engine parameters

i. number of cylinders

ii. cylinder bore and stroke

iii. clearance volume

iv. connecting rod length

v. valve timings (crank angles at which the intake and exhaust valves open and close)

vi. tabulated values for the valve open areas and discharge coefficients

b. Other component dimensions

i. manifold dimensions

ii. connecting passage dimensions

iii. EGR and wastegate valve dimensions

iv. wastegate actuator characteristics

c. Intercooler characteristics

i. coolant flow heat capacity

ii. heat exchange surface area

iii. heat exchanger heat transfer coefficient

d. Turbomachinery parameters

i. turbocharger rotational inertia

ii. turbocharger rotational damping

iii. power turbine gear ratio

iv. power turbine transmission efficiency

v. compressor, turbine and power turbine maps

(see Sec. 11.2 - Turbocharger and power turbine maps)

11.1.3 Heat transfer and turbulent flow parameters

a. constants for the Nusselt-Reynolds number correlation

b. the temperatures of the piston, cylinder head, cylinder walls and manifold walls

c. the turbulent dissipation constant

11.1.4 Engine friction parameters

Empirical constants associated with the calculation of friction losses

11.1.5 Initial conditions

a. intake manifold pressure and temperature

b. exhaust manifold pressure and temperature

c. turbocharger speed

11.1.6 Ambient conditions

a. intake temperature

b. intake pressure

c. final exhaust pressure

11.1.7 Computational parameters

a. convergence margins for each state variable

b. error tolerances for integration of the differential equations

c. other parameters used in the integration algorithm

(For a detailed description of these parameters, see the engine simulation code.)

11.2 Turbocharger and Power Turbine Maps

Maps give the interrelationships among mass flow rate, efficiency, pressure ratio and rotor speed for each of the three turbomachinery components: turbocharger compressor and turbine, and power turbine. The maps are put into the simulation in tabular form and must therefore be reduced to tabular form if initially in graphical form. The tables are interpolated during the simulation to find the necessary information. The map variables of mass flow rate and rotor speed are corrected by factors relating actual inlet conditions to standard conditions. The speed correction factor involves inlet temperature, and the mass flow rate correction factor involves inlet temperature and pressure.

The compressor map variables are 1) $\dot{m}_c$, 2) p_2/p_1 3) η_c and 4) ω. The mass flow rate is normalized according to p_8 and T_8. The rotor speed is normalized according to T_8.

The turbine map variables are 1) $\dot{m}_t$, 2) p_8/p_9, 3) η_t and 4) ω.

The mass flow rate is normalized according to p_8 and T_8. The rotor speed is normalized according to T_8.

The power turbine map variables are 1) $\dot{m}_{pt}$, 2) p_{10}/p_{11}, 3) η_{pt}, 4) ω_{pt}. Mass flow rate is normalized according to p_{10} and T_{10}. The shaft speed, which is directly determined from the engine speed and the specified gear ratio, is normalized according to T_{10}.

11.3 Outputs

Four types of outputs are generated by the cycle simulation:

11.3.1 Input echo

A listing of all the input parameters, including some quantities derived directly from the given inputs (e.g. engine displacement and compression ratio)

11.3.2 Major crank-angle by crank angle results

At specified crank-angle intervals, the values of the following state variables are returned:

a. cylinder pressure, temperature, and average equivalence ratio

b. intake manifold pressure, temperature and average equivalence ratio

c. exhaust manifold pressure, temperature and average equivalence ratio

d. turbocharger speed

In addition, the following other quantities are reported at the same intervals:

a. engine total heat transfer rate

b. heat transfer rates to different surfaces of interest

c. engine work done

d. turbulent flow model results (such as mean flow velocity, turbulent

d. turbulent flow model results (such as mean flow velocity, turbulent intensity, macroscale of turbulence)

e. a code which monitors the performance of the integration routine

Integrating through the different processes for the master cylinder, the following quantities are reported during the corresponding process:

a. Intake

i. mass flows through each valve

ii. mass fraction of fresh charge (air) in the cylinder

b. Combustion

i. a non-dimensional fuel burning rate

ii. fuel burnt as a function of total fuel injected

c. Exhaust

i. mass flow rate and velocity through exhaust valve

11.3.3 Integrated results and cycle performance

After completion of an engine cycle, a summary of results obtained by integrating some of the governing equations over the cycle is given. Integrated results include the following:

a. volumetric and thermal efficiencies

b. gross indicated, pumping and friction mean effective pressures

c. total heat loss

d. ignition delay period

e. estimated mean exhaust temperature

f. mass in cylinder at IVO and at IVC

g. mass of air inducted per cycle

h. total heat and work transferred during each process

i. results of an overall energy balance

11.3.4 Sub-model results

After the overall cycle results are listed, detailed results for the main sub-models of the cycle simulation are given at specified crank angle intervals. These quantities include the following:

a. total engine intake and exhaust mass flow rates

b. compressor, turbocharger turbine and power turbine mass flow rates, pressure ratios and efficiencies

c. wastegate (turbocharger turbine bypass) and EGR mass flow rates

d. power turbine work transfer

e. pressures and temperatures at various system locations

f. intake and exhaust manifold heat transfer rates

g. intercooler effectiveness

12. REFERENCES

1. Katz, N.R. and Lenoe, E.M., "Ceramics for Diesel Engines: Preliminary Results of a Technology Assessment," Progress Report DOE/AMMRC IAG DE-AE 101-77 CS51017, 1981.

2. Kamo, R. and Bryzik, W., "Adiabatic Turbocompound Engine Performance Predictions," SAE Paper 780068, 1978.

3. Kamo, R. and Bryzik, W., "Cummins-TARADCOM Adiabatic Turbocompound Engine Program," SAE paper 810070, 1981.

4. Poulos, S.G. and Heywood, J.B., "The Effect of Chamber Geometry on Spark-Ignition Engine Combustion," SAE paper 830334, 1983.

5. Mansouri, S.H., Heywood, J.B. and Radhakrishnan, K., "Divided-Chamber Diesel Engines, Part 1: A Cycle-Simulation which Predicts Performance and Emissions," SAE Paper 820273, 1982.

6. Watson, N. and Janota, M.S., Turbocharging the Internal Combustion Engine, John Wiley & Sons, New York, 1982.

7. Lyn, W.T., "Study of Burning Rate and Nature of Combustion in Diesel Engine," IX Symposium (International) on Combustion, Proceedings, pp. 1069-1082, The Combustion Institute, 1962.

8. Shipinski, J., Uyehara, O.A. and Myers, P.S., "Experimental Correlation Between Rate-of-Injection and Rate-of-Heat-Release in a Diesel Engine," ASME Paper 68-DGP-11, 1968.

9. Watson, N., Pilley, A.D. and Marzouk, M., "A Combustion Correlation for Diesel Engine Simulation," SAE Paper 800029, 1980.

10. Hardenberg, H.O. and Hase, F.W., "An Empirical Formula for Computing the Pressure Rise Delay of a Fuel from its Cetane Number and from the Relevant Parameters of Direct-Injection Diesel Engines," SAE paper 790493, 1979.

11. Dent, J.C. and Mehta, P.S., "Phenomelogical Combustion Model for a Quiescent Chamber Diesel Engine," SAE Paper 811235, 1981.

12. Woschni, G., "A Universally Applicable Equation for the Instantaneous Heat Transfer Coefficient in the Internal Combustion Engine," SAE Paper 670931, 1967.

13. Annand, J.D., "Heat Transfer in the Cylinders of Reciprocating Internal Combustion Engines," Proceedings Institute of Mechanical Engineers, Vol. 177, No. 36, 1963.

14. Annand, J.D. and Ma, T.H., "Instantaneous Heat Transfer Rates to the Cylinder Head Surface of a Small Compression-Ignition Engine," Proceedings Institute of Mechanical Engineers, Vol. 185, No. 72, 1971.

15. Sitkei, G., "Heat Transfer and Thermal Loading in Internal Combustion Engines," Akademiai Kiade, Budapest, 1974.

16. Kamel, M. and Watson, N., "Heat Transfer in the Indirect Injection Diesel Engine," SAE Paper 790826, 1979.

17. Oguri, T. and Shigewo, I., "Radiant Heat Transfer in Diesel Engines," SAE paper 720023, 1972.

18. Kunitomo, T., Matsuoka, K. and Oguri, T., "Prediction of Radiative Heat Flux in a Diesel Engine," SAE Paper 750786, SAE Trans., Vol. 84, 1975.

19. Tennekes, M. and Lumley, J.L., A First Course in Turbulence, M.I.T. Press, Cambridge, Mass., 1972.

20. Millington, B.W. and Hartles, E.R., "Frictional Losses in Diesel Engines," SAE paper 680590, 1968.

21. Hires, S.D., Ekchian, A., Heywood, J.B., Tabaczynski, R.J. and Wall, J.C., "Performance and NO_x Emissions Modelling of a Jet Ignition Prechamber Stratified Charge Engine," SAE Paper 760161, 1976.

22. Martin, M.K. and Heywood, J.B., "Approximate Relationships for the Thermodynamic Properties of Hydrocarbon-Air Combustion Products," Combustion Science and Technology, Vol. 15, pp. 1-10, 1977.

23. Svehla, R.A. and McBride, B.J., "Fortran IV Computer Program Calculations of Thermodynamic and Transport Properties of Complex Chemical Systems," NASA Technical Note, NASA TN D-7056, 1973.

24. Mansouri, S.H. and Heywood, J.B., "Correlations for the Viscosity and Prandtl Number of Hydrocarbon-Air Combustion Products," Combustion Science and Technology, Vol. 23, pp. 251-256, 1980.

25. Kays, W.M., London, A.L. and Johnson, D.W., "Gas Turbine Plant Heat Exchangers," ASME, New York, 1951.

26. Rohsenow, W.M. and Choi, H.Y., Heat, Mass, and Momemtum Transfer, Prentice-Hall, Englewood Cliffs, N.J., 1961.

27. Shampine, L.F. and Gordon, M.K., Computer Solution of Ordinary Differential Equations: The Initial Value Problem, Freeman, 1974.

Table I: Constants for Arrhenius Equation for Ignition Delay [ms]

Fuel	Cetane No.	A	n	E/R kelvins	Ref.	Notes
diesel		53.5	1.23	676.5	(a)	
n-cetane	100	0.872	1.24	4050	(a)	Bomb data at high pressure
n-heptane		0.748	1.44	5270	(a)	
diesel	45-50	4.05×10^{-2}	0.757	5470	(b)	Steady flow reactor
diesel		2.43×10^{-6}	2	20915.3	(c)	
kerosene		1.68×10^{-5}	2	19008.7	(c)	Continuous flow apparatus
cetane		4.04×10^{-10}	2	25383	(c)	
diesel		3.45	1.02	2100	(d)	

(a) Igura, S., Kadota, T., Hirozasu, H., "Spontaneous Ignition Delay of Fuel Sprays in High Pressure Gaseous Environment," Jap. Soc. Mech. Engrs., Vol. 41, No. 345, p. 1559, (1975).

(b) Stringer, F.W., Clarke, A.E., Clarke, J.S., "The Spontaneous Ignition of Hydrocarbon Fuels in a Flowing System," Proc. Auto. Div., Institution of Mech. Eng., 1970.

(c) Spadaccini, L.J., and TeVelde, J.A., "Autoignition Characteristics of Aircraft-Type Fuels," United Technologies Research Center, NASA report CR-159886, 1980.

(d) Watson, N., Pilley, A.D. and Marzouk, M., "A Combustion Correlation for Diesel Engine Simulation," SAE paper 800029, 1980.

Table II: Burned Gas Composition under 1000°K

x_i (moles/moleO_2 reactant)

i	Species	$\phi \leq 1$	$\phi > 1$
1	CO_2	$\varepsilon\phi$	$\varepsilon\phi$ -C
2	H_2O	$2(1-\varepsilon)\phi$	$2(1-\varepsilon\phi)$ + C
3	CO	0	C
4	H_2	0	$2(\phi-1)$ - C
5	O_2	$1 - \phi$	0
6	N_2	ψ	ψ
	sum	$(1-\varepsilon)\phi + 1 + \psi$	$(2-\varepsilon)\phi + \psi$

Table III: Coefficients for Polynomial Fit to Thermodynamic Properties

Coefficients for 100°K < T ≤ 500°K

i	Species	a_{i1}	a_{i2}	a_{i3}	a_{i4}	a_{i5}	a_{i6}*
1	CO_2	4.7373	16.653	-11.232	3.8280	.006767	-93.75793
2	H_2O	7.8097	-.20235	3.4187	-1.1790	.001436	-57.08004
3	CO	6.9739	-.82383	2.9420	-1.1762	.0004132	-27.19597
4	H_2	6.9919	.16170	-.21821	.29682	-.016252	-.118189
5	O_2	6.2957	2.3884	-.031479	-.32674	.004359	.103637
6	N_2	7.0922	-1.2958	3.2069	-1.2022	-.0003458	-.013967

Coefficients for 500°K < T < 6000°K

i	Species	a_{i1}	a_{i2}	a_{i3}	a_{i4}	a_{i5}	a_{i6}*
1	CO_2	11.940	2.0886	-.47029	.037363	-.58945	-97.1418
2	H_2O	6.1391	4.6078	-.93560	.066695	.033580	-56.62588
3	CO	7.0996	1.2760	-.28775	.022356	-.15987	-27.73464
4	H_2	5.5557	1.7872	-.28813	.019515	.16118	.76498
5	O_2	7.8658	.68837	-.031944	-.0026870	-.20139	-.893455
6	N_2	6.8078	1.4534	-.32999	.025610	-.11895	-.331835

* picked to give enthalpy datum at 0°K

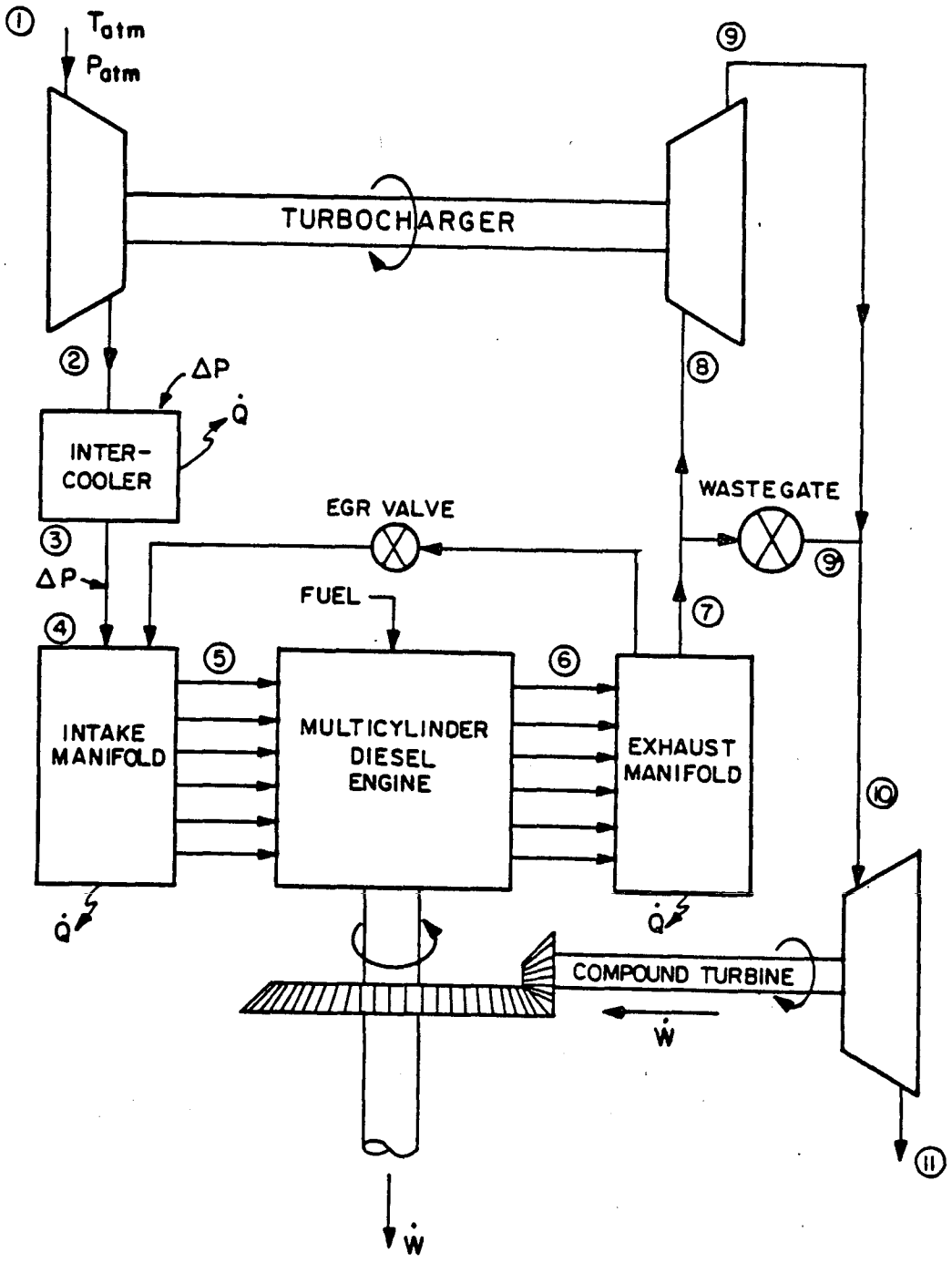

Figure 1: Turbo-compounded diesel system configuration

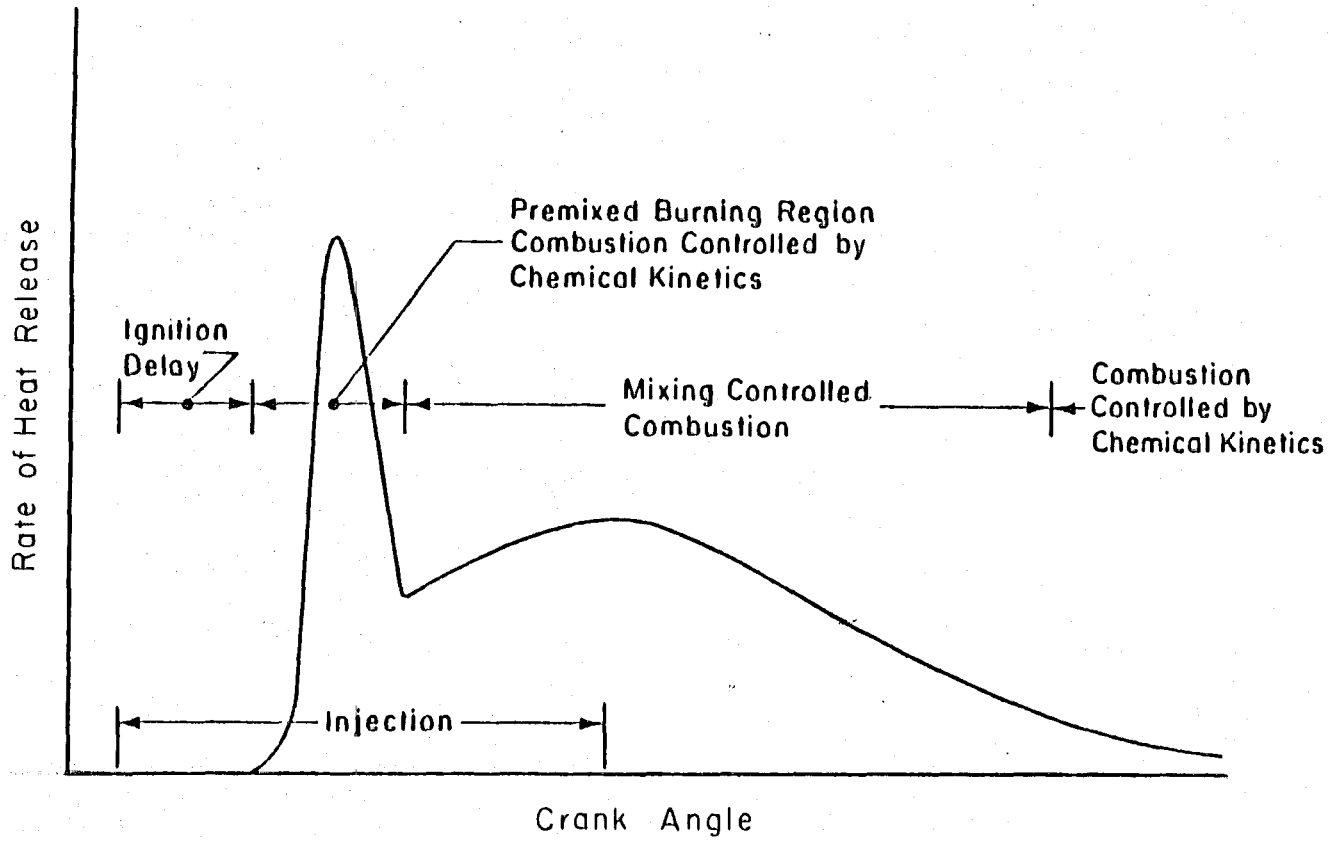

Figure 2: Typical rate of heat release diagram for a DI diesel engine

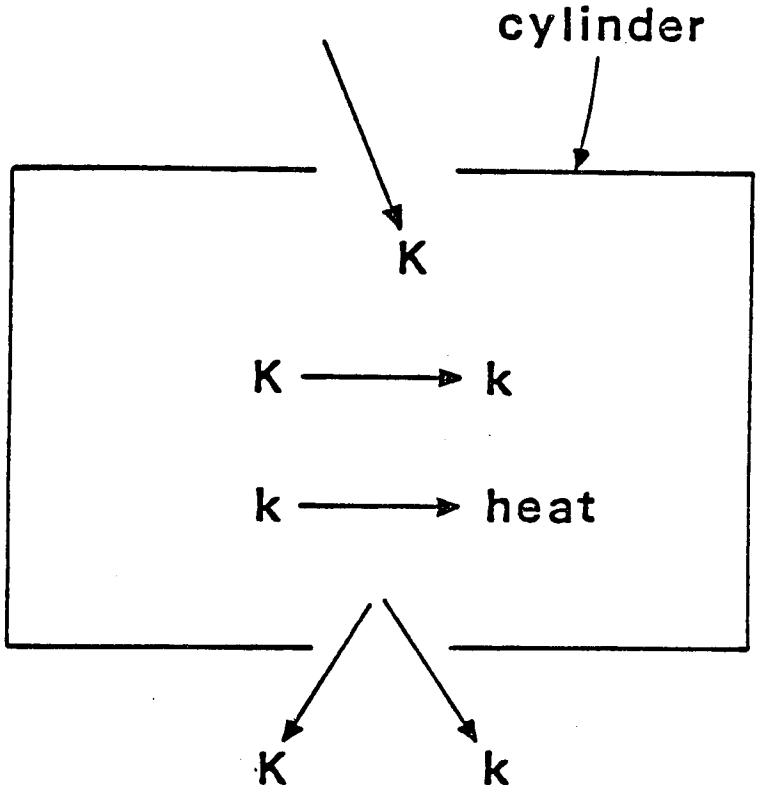

Figure 3: Energy cascade model

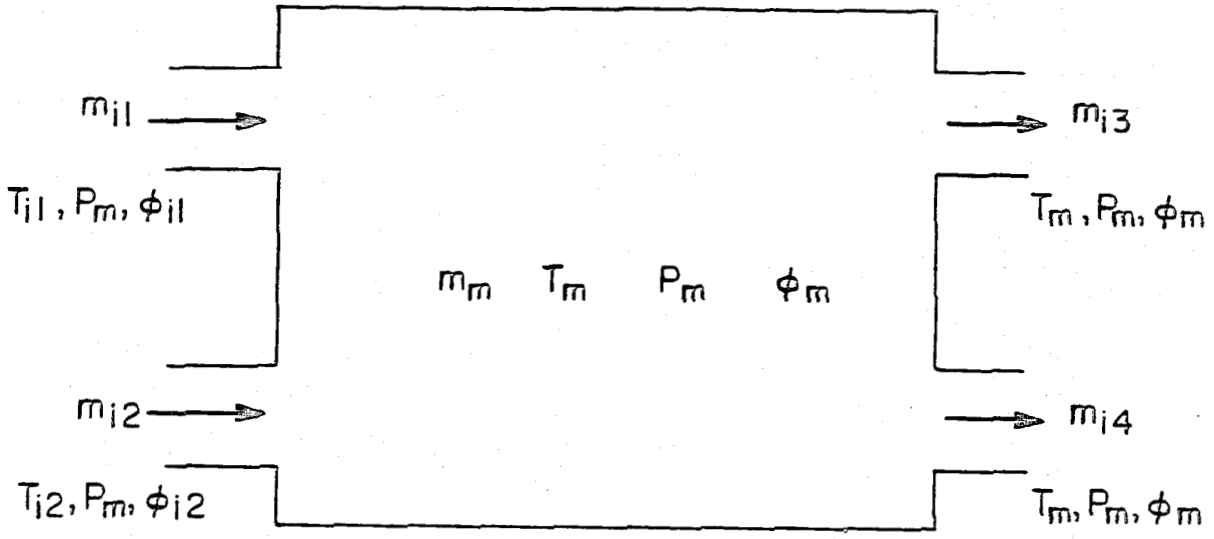

Figure 4: General manifold control volume

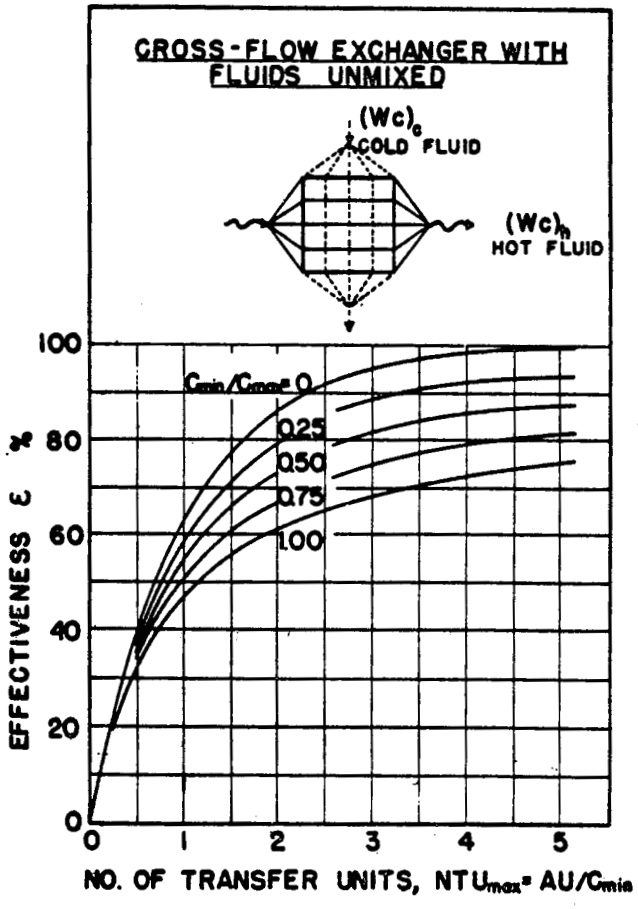

Figure 5: Cross-flow heat exchanger effectiveness vs. NTU

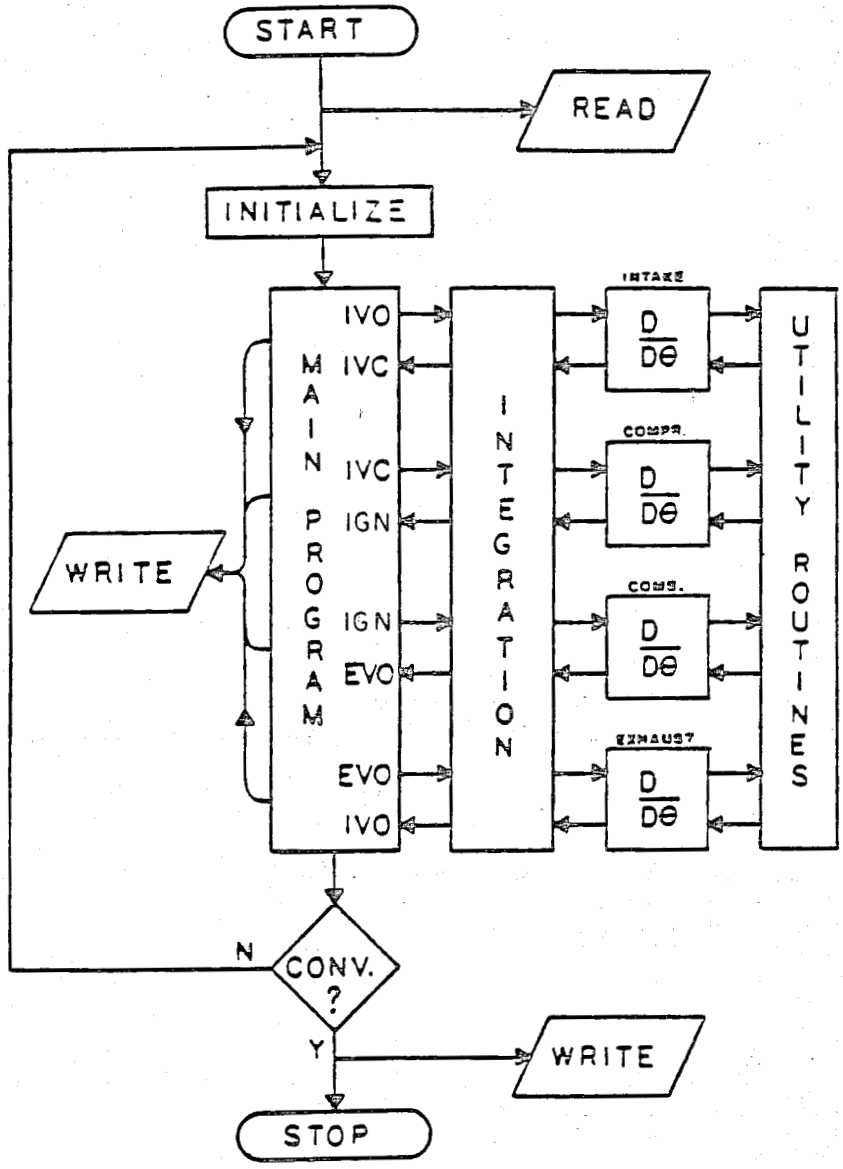

Figure 6: Flowchart of simulation program

1. Report No.	2. Government Accession No.	3. Recipient's Catalog No.
NASA CR-174755		

4. Title and Subtitle	5. Report Date
Computer Simulation of the Heavy-Duty Turbo-Compounded Diesel Cycle for Studies of Engine Efficiency and Performance	May 1984
	6. Performing Organization Code
7. Author(s)	8. Performing Organization Report No.
Dennis N. Assanis, Jack A. Ekchian, John B. Heywood, and Kriss K. Replogle	
	10. Work Unit No.
9. Performing Organization Name and Address	11. Contract or Grant No.
Sloan Automotive Laboratory Massachusetts Institute of Technology Cambridge, Massachusetts 02139	NAG 3-394
	13. Type of Report and Period Covered
12. Sponsoring Agency Name and Address	Contractor Report
U.S. Department of Energy Office of Vehicle and Engine R&D Washington, D.C. 20585	14. Sponsoring Agency ~~Code~~ Report No. DOE/NASA/0394-1

15. Supplementary Notes

Interim Report. Performed under Interagency Agreement DE-AI01-80CS50194. Project Manager, James C. Wood, Transportation Propulsion Division, NASA Lewis Research Center, Cleveland, Ohio 44135.

16. Abstract

It has been shown that reductions in heat loss at appropriate points in the diesel engine result in substantially increased exhaust enthalpy. One of the promising concepts for taking advantage of this increased enthalpy is the turbocharged, turbo-compounded diesel engine cycle. In 1983 the Department of Energy sponsored a program for a computer simulation of the heavy duty turbocharged, turbo-compounded diesel engine system. This would enable the engineer to define the tradeoffs associated with introducing ceramic materials in various parts of the total engine system, and to carry out system optimization studies. This report describes the basic assumptions and the mathematical relationships used in the simulation of the model engine.

17. Key Words (Suggested by Author(s))	18. Distribution Statement
Diesel engine Transportation Computer model Energy Fuel consumption	Unclassified - unlimited STAR category 85

19. Security Classif. (of this report)	20. Security Classif. (of this page)	21. No. of pages	22. Price*
Unclassified	Unclassified	65	A04

*For sale by the National Technical Information Service, Springfield, Virginia 22161